Published in final edited form as:

Nat Med. 2017 February ; 23(2): 164–173. doi:10.1038/nm.4262.

Loss of μ-opioid receptor signaling in nociceptors, and not spinal microglia, abrogates morphine tolerance without disrupting analgesic efficacy

Gregory Corder[1,2,3,4,9], **Vivianne L. Tawfik**[1,2,3,4,9], **Dong Wang**[1,2,3,4,9], **Elizabeth I. Sypek**[1,5,9], **Sarah A. Low**[1,2,3,4], **Jasmine R. Dickinson**[1,6], **Chaudy Sotoudeh**[1,2,3,4], **J. David Clark**[1,8], **Ben A. Barres**[4,7], **Christopher J. Bohlen**[4,7], and **Grégory Scherrer**[1,2,3,4,*]

[1]Department of Anesthesiology, Perioperative and Pain Medicine, Stanford University, Stanford, CA 94305, USA

[2]Department of Molecular and Cellular Physiology, Stanford University, Stanford, California, USA

[3]Department of Neurosurgery, Stanford University, Stanford, CA 94305, USA

[4]Stanford Neurosciences Institute, Stanford, CA 94305, USA

[5]Stanford University Neuroscience Graduate Program, Stanford, CA 94305, USA

[6]Stanford University Biology Graduate Program, Stanford, CA 94305, USA

[7]Department of Neurobiology, Stanford University, Stanford, CA 94305, USA

[8]Anesthesiology Service, Veteran's Affairs Palo Alto Health Care System, Palo Alto, CA 94304, USA

Abstract

Opioid pain medications cause detrimental side effects including analgesic tolerance and opioid-induced hyperalgesia (OIH). Tolerance and OIH counteract opioid analgesia, and drive dose escalation. The cell-types and receptors on which opioids act to initiate these maladaptive processes remain disputed, preventing the development of therapies to maximize and sustain opioid analgesic efficacy. Here we establish that mu-opioid receptors (MOR) expressed by primary afferent nociceptors initiate tolerance and OIH development. RNA-sequencing and histological analysis revealed that MOR is expressed by nociceptors, but not by spinal microglia. Deletion of MOR specifically in nociceptors eliminated morphine tolerance, OIH, and

*Correspondence should be addressed to G.S. (gs25@stanford.edu).

[9]These authors contributed equally to this work

AUTHOR CONTRIBUTIONS

G.C. and J.R.D. designed and performed behavioral pharmacology. G.C., V.L.T., D.W., E.I.S., S.A.L., and C.S. performed histology. D.W. performed spinal cord slice electrophysiology. E.I.S., C.J.B., and B.A.B. designed and performed RNA transcriptome sequencing. J.D.C. provided critical input on study design and interpretation. G.C., V.L.T., D.W., E.I.S., and G.S. designed studies and wrote the manuscript. All authors contributed to data analysis and editing of the manuscript. G.S. supervised all experiments. The project was conceived by G.C., V.L.T., D.W. and G.S.

COMPETING FINANCIAL INTERESTS

There is NO Competing Interest.

pronociceptive synaptic long-term potentiation, without altering antinociception. Furthermore, we found that co-administration of methylnaltrexone bromide, a peripherally restricted MOR antagonist, is sufficient to abrogate morphine tolerance and OIH without diminishing antinociception in perioperative and chronic pain models. Collectively, our data support combining opioid agonists with peripheral MOR antagonists to limit analgesic tolerance and OIH.

INTRODUCTION

Opioid analgesics, such as morphine, continue to be the mainstay to manage severe, perioperative and chronic pain[1,2]. With the staggering prevalence of pain[3], the broad use of opioids for pain management has increased dramatically in the past decades. In the United States, this increase in opioid prescriptions has been accompanied by a sharp rise in the incidence of addiction and opioid-related mortality, a phenomenon termed the Opioid Epidemic[4]. Chronic opioid use can result in analgesic tolerance, where analgesic efficacy gradually decreases at fixed drug doses, and paradoxical opioid-induced hyperalgesia (OIH)[5]. Tolerance and OIH are primary drivers of diminished pain control and dose escalation[6,7], and novel therapeutic strategies that would bolster opioid analgesia while mitigating tolerance and OIH are urgently required to improve patients' safety.

While opioid analgesia results from binding and signaling through mu opioid receptors (MORs)[8] present along pain neural circuits[9], the cell-types and receptors mediating tolerance and OIH remain disputed[10,11]. Tolerance and OIH are adaptive processes proposed to result from complex alterations at the molecular level for MOR, as well as at the synaptic, cellular, and circuit levels, in both the peripheral and central nervous systems[12,13]. Thus, chronic opioids modify neuronal MOR function, including via receptor phosphorylation, signaling, multimerization, and trafficking, which may underlie tolerance and OIH[12,14]. Other studies suggest that glial cells, and in particular microglia, are essential contributors to opioid tolerance and OIH[15]. Chronic opioids cause microglia and astrocyte activation, and interfering with glial function has been shown to reduce tolerance and OIH[16,17]. Mechanistically, previous studies have proposed that glial cells express MOR, and that opioid binding to this MOR population activates microglia[10]. However, unequivocal evidence for MOR expression in microglia is lacking[18], and other studies support the idea that morphine binds and activates TLR4 and MD-2 signaling in microglia[17,19]. Adding to the controversy, recent reports indicated no change in tolerance and OIH in TLR4 knockout (KO) mice[20,21]. Consequently, the contributions of neuronal versus glial cells, and the molecular mechanisms initiating analgesic tolerance and OIH, remain unresolved.

Opioids alter the properties of MOR-expressing neurons and connected nociceptive circuits at the level of the dorsal root ganglia (DRG), spinal cord dorsal horn, and brain (including in the brainstem descending pain control systems)[12,13]. MOR function in primary afferent nociceptors is of particular interest as an initiation site for tolerance and OIH, as this cell-type has been implicated in the development of antinociceptive tolerance, physical dependence, and the pronociceptive effects of opioids[5,22,23] (Supplementary Note 1). Indeed, nociceptors undergo and drive pronociceptive plasticity, in downstream CNS circuits during persistent pain[24,25]. Electrophysiological studies have demonstrated that opioids not

only depress neurotransmission between nociceptors and dorsal horn neurons[26], but can also generate maladaptive plasticity, such as long-term potentiation (LTP)[27]. Opioid-induced LTP is now considered a critical neural substrate for OIH[24], and may contribute to tolerance. The pre-[28] versus post-[27] synaptic origin of opioid-induced LTP is presently debated, and whether LTP is initiated by MOR activation in nociceptors or spinal neurons is not known. Interestingly, previous reports indicated that ablation of TRPV1 nociceptors not only abolishes opioid-induced LTP[28], but also reduces tolerance and OIH[29]. Because we and others have shown that in DRG MOR is predominantly expressed by peptidergic TRPV1 nociceptors[30,31] we tested here the hypothesis that MOR expressed by nociceptors represents a critical and susceptible element within nociceptive circuits for the initiation of maladaptive mechanisms driving analgesic tolerance and OIH.

RESULTS

Morphine tolerance and OIH, but not microglial activation, requires MOR

We first determined whether morphine tolerance and OIH could be dissociated from microglial activation by examining, in parallel, the consequences of morphine treatment on microglial activation, antinociceptive tolerance, and OIH, in wild-type control and global MOR KO mice. In wild-type mice, chronic morphine treatment produced significant antinociceptive tolerance and OIH (Figure 1a,b; Supplementary Figure 1), as well as robust microglial activation as evidenced by increased CD11b density (Figure 1c,d), with either a fixed once daily 10 mg/kg dose, or with a twice daily escalating 10 to 40 mg/kg schedule. Strikingly, we found that global MOR KO mice treated with the escalating morphine schedule showed considerable microglial activation, but no OIH (Figure 1b–d).

Microglia lack *Oprm1* mRNA transcript, tagged-MOR protein, and MOR-immunoreactivity

To further investigate the mechanistic separation between OIH and microglial activation, we utilized immunohistochemistry (IHC), *in situ* hybridization (ISH), and knockin mice expressing a fluorescent tagged receptor (MOR-mCherry), to establish which cellular populations express MOR. We found that MOR is expressed in nociceptive neurons in DRG and spinal cord dorsal horn (Supplementary Figures 2 and 3). However, examination of dorsal horn sections provided no clear evidence for *Oprm1* mRNA transcripts, anti-MOR immunoreactivity, or MOR-mCherry expression in microglia, identified by CX3CR1-GFP or CD11b immunoreactivity (Figure 1e–g and Supplementary Figure 4). Because these results could be explained by the relatively limited sensitivity of histological and imaging techniques, we performed RNA-sequencing (RNA-seq) transcriptome profiling on acutely purified, non-cultured spinal microglia from adult mice. We analyzed expression of exons encoding the canonical seven transmembrane MOR, as well as that of alternative splice variants and truncated receptors[32]. Unlike in DRG, we did not detect any *Oprm1* transcript in purified spinal microglia (Figure 1h). RNA-seq reads were mapped within the oppositely oriented *Ipcef1* gene, which partially overlaps with *Oprm1*, but no reads aligned to exons 1 – 4 of *Oprm1* (which are required for the expression of the canonical seven transmembrane protein[32]). Microglial *Oprm1* transcripts mapping to exons 1 – 4 were also undetectable in mice with chronic neuropathic pain (Figure 1i and Supplementary Figure 5 and Supplementary Note 2), or treated with chronic morphine (Supplementary Figure 6). We

propose that MOR action in neurons likely drives the initiation of opioid nociceptive side effects.

Genetic deletion of MOR from nociceptors does not reduce systemic morphine antinociception

We next sought to identify the specific population of MOR+ neurons that promote morphine analgesia, as well as those initiating tolerance and OIH. Because it is difficult to probe the specific function of pre- and post-synaptic MOR populations using traditional pharmacological approaches, we took advantage of mouse genetic engineering. We generated conditional knockout mice lacking MOR in neurons of the TRPV1 lineage (MOR cKO mice). Mice bearing alleles in which exons 2 and 3 of the *Oprm1* gene are floxed were crossed with knockin mice in which expression of Cre recombinase is driven by the promoter of the *Trpv1* gene (Figure 2a). TRPV1 is largely restricted to peptidergic nociceptors in adult mice, but is also expressed in non-peptidergic and myelinated nociceptors earlier during development[33], resulting in Cre-mediated recombination in the great majority of nociceptors (Supplementary Figure 7). Consequently, the *Oprm1* gene is excised selectively in DRG, and not spinal cord or brain in MOR cKO mice (Figure 2b and Supplementary Figure 8). Thus, fluorescence ISH and IHC experiments indicated that *Oprm1* expression is found only in 6.3% (ISH) and 4.2% (IHC) of DRG neurons in MOR cKO mice, compared to 42.6% (ISH) and 38.7% (IHC) in littermate controls (Figure 2c–f). In the spinal cord, MOR immunoreactivity was strongly decreased in the dorsal horn CGRP + laminae I and II outer (Figure 2g–j), while a faint MOR signal persisted in the IB4+ lamina II inner (Figure 2k,l), where MOR is expressed in spinal interneurons[34].

Clinically, opioids provide substantive relief of both sensory and affective dimensions of the pain experience. Therefore, we next evaluated basal nociception, and morphine antinociception, in MOR cKO mice, monitoring both nociceptive sensory-reflexive and affective-motivational behaviors (see *Online Methods*). MOR cKO mice exhibited similar basal nociceptive reflexes and affective-motivational responses to thermal and mechanical stimuli, relative to littermate controls (Figure 2m–o). Importantly, while acute intrathecal morphine (1 μg) generated robust antinociception in control mice, intrathecal morphine did not produce significant reflexive or affective-motivational antinociception in MOR cKO mice (Figure 2p–r), revealing that spinal opioid antinociception primarily results from presynaptic MOR signaling in nociceptors[35]. In contrast, subcutaneous morphine (10 mg/kg) produced maximal reflexive and affective-motivational antinociception in MOR cKO mice (Figure 2s–u and Supplementary Note 3).

Morphine action at nociceptor MORs underlies tolerance and OIH initiation

We next evaluated the development of morphine antinociceptive tolerance and OIH in MOR cKO mice. We treated mice with systemic, fixed-dose morphine (10 mg/kg, subcutaneous) once daily for 10 days. We measured thermal and mechanical nociceptive thresholds, and affective-motivational responses to noxious thermal stimuli prior to, and 30 min after, each daily injection, to evaluate OIH and tolerance, respectively (Figure 3a,d,g). Remarkably, we found that while morphine antinociception progressively diminished in littermate controls, morphine retained near full antinociceptive efficacy across all days in MOR cKO mice

(Figure 3b,e,h). Moreover, MOR cKO mice developed significantly less OIH than controls for thermal and mechanical stimuli (Figure 3c,f,i). This result suggests that chronic opioid action at MOR expressed by nociceptors triggers the onset of pronociceptive maladaptive plasticity that results in analgesic tolerance and OIH.

Opioids induce a MOR-dependent, pre-synaptic form of spinal LTP

Opioids not only acutely depress synaptic transmission in the spinal cord[35], but also trigger excitatory plasticity mechanisms[36,37], such as LTP[27]. It is presently unclear whether opioid-induced LTP is initiated by activation of presynaptic or postsynaptic MOR signaling mechanisms. To address this question, we interrogated synaptic transmission between nociceptors and spinal neurons using spinal cord slices from MOR cKO mice and littermate controls expressing the light-activated channel channelrhodopsin 2 (ChR2) in TRPV1 nociceptors. Immunohistochemical studies confirmed expression of ChR2-eYFP in peptidergic DRG nociceptor somata and their terminals in lamina I and II outer (Figure 4a,b). We made whole-cell recordings from lamina I – II outer neurons with monosynaptic input from ChR2-expressing nociceptors. Bath application of the MOR agonist [D-Ala^2, N-MePhe^4, Gly-ol^5]-enkephalin (DAMGO; 500 nM) for 5 min induced a rapid depression of light–evoked excitatory postsynaptic currents (EPSCs) in all 15 recorded neurons (52 ± 10.5% inhibition at 5 min of application) (Figure 4c). Thirty minutes after washout of DAMGO, EPSC amplitudes were potentiated to 142.2 ± 6.1% of control in 8 out of 15 neurons (Figure 4c and Supplementary Figure 9), consistent with previous reports[27,28]. This opioid-induced LTP persisted for the duration of the recording. Strikingly, we found that both DAMGO-induced inhibition and LTP were completely lost in 9 out of 9 recorded neurons from MOR cKO mice (DAMGO inhibition: 98 ± 8.12% of control; DAMGO-washout: 96.2 ± 11.9%) (Figure 4d). Collectively, these results establish that presynaptic MOR signaling in TRPV1 nociceptors is essential to maladaptive spinal opioid-induced LTP.

Peripheral MOR blockade prevents the onset of morphine tolerance and OIH

Our genetic *Oprm1* conditional deletion strategy demonstrates that loss of MOR signaling in DRG nociceptors prevents the onset of morphine antinociceptive tolerance and OIH. We reasoned that pharmacological blockade of peripheral MOR might similarly alleviate these opioid side effects. In wild-type C57Bl/6J mice, we paired injections of subcutaneous morphine with methylnaltrexone bromide (MNB), a blood-brain barrier impermeable MOR antagonist[38]. We assessed the antinociceptive effects of morphine and MNB combination therapy on nociceptive reflexes and affective-motivational behaviors. We used a paradigm in which the noxious environment cannot be escaped (Figure 5a–e and Supplementary Figure 10), in addition to monitoring pain-like behaviors elicited by acute, punctate mechanical, and noxious thermal stimuli (Figure 5f–k). We found that morphine significantly reduced nociceptive reflexes (Figure 5a,b,c,f and Supplementary Figure 11a–d), and was effective at alleviating affective-motivational behaviors (Figure 5a,d,e,g and Supplementary Figure 11a,e–m). The combination treatment with MNB (0.1 – 10.0 mg/kg) did not alter morphine antinociceptive effects (Figure 5a,b,d,f,g, Supplementary Figure 11 and Supplementary Note 4), consistent with our result in MOR cKO mice. We next determined whether MNB can effectively prevent opioid antinociceptive tolerance and OIH, by treating mice with a fixed combination of morphine (10 mg/kg) and MNB (0.1 – 10.0 mg/kg), or morphine alone, once

daily for 7 days (Figure 5a–k). Remarkably, while mice treated with morphine alone developed robust antinociceptive tolerance and OIH on both reflexive and affective-motivational measures on Day 7 compared to Day 1 morphine antinociception and pre-morphine baseline levels, we found that mice co-treated with morphine plus MNB showed a dose-dependent reduction in the onset of tolerance and OIH (Figure 5a–k and Supplementary Figure 12). The administration of MNB combination therapy did not produce any behavioral symptoms of physical withdrawal at any of the tested doses.

MNB and morphine combination therapy provides long-lasting relief from chronic pain

Clinically, opioids are prescribed for managing both perioperative and chronic pain. Therefore, we next assessed the antinociceptive efficacy of morphine and MNB combination therapy in these persistent pain states. We used a tibia fracture and bone pinning model of orthotrauma inflammatory pain and found that while morphine alone (10 mg/kg) acutely produced antinociception, morphine was no longer effective at reducing nociceptive or affective-motivational orthotrauma pain after 7 days of chronic treatment (Figure 6a,b,d,e). In contrast, morphine (10 mg/kg) and MNB (10 mg/kg) combination therapy produced strong antinociception against mechanical reflexive hypersensitivity, as well as against affective-motivational pain responses, with no indication of tolerance (Figure 4a,b,d,e and Supplementary Figure 13a,b). Furthermore, no OIH was observed during prolonged use of the combination therapy (Figure 6a,c,d,f and Supplementary Figure 13c). Similarly, morphine and MNB combination therapy prevented the development of antinociceptive tolerance in the chronic constriction injury (CCI) model of neuropathic chronic pain (Figure 6g–l). We did not observe indications of OIH in the control group (CCI + morphine alone), possibly due to floor and/or ceiling effects (Figure 6i,l). Together, these pharmacological results uncover the potential benefit of a peripherally restricted opioid antagonist to limit detrimental pronociceptive side effects that accompany prolonged opioid use.

DISCUSSION

Our study identifies opioid signaling through MOR on primary afferent nociceptors, and not spinal microglia, as the critical molecular event initiating maladaptive plasticity within nociceptive neural circuits, resulting in analgesic tolerance and OIH. The properties of several cell-types and circuits in which MOR is present are altered following chronic opioid treatments, including at the level of DRG nociceptors, spinal neurons, spinal microglia, brainstem nuclei, and sub-cortical and cortical brain regions (Supplementary Note 1). We propose that morphine-induced sensitization of MOR-expressing nociceptors facilitates downstream plasticity in CNS pain and analgesia circuits that promote the development and maintenance of OIH and tolerance (Figure 6m,n and Supplementary Note 5). Thus, elimination of peripheral MOR signaling permits central opioid action to retain analgesic efficacy.

Non-selective pharmacological glial inhibitors, such as minocycline and propentofylline, are well documented to attenuate opioid tolerance in rodents[16,17], and morphine has been recently proposed to act on MOR expressed by microglia to activate these cells and initiate OIH[10]. Using multiple histological approaches and highly sensitive RNA-seq of non-

cultured, acutely purified adult spinal microglia, we did not find compelling evidence supporting MOR expression in microglia, contrary to previous findings from *in vitro*[39,40] and *in vivo* studies[10,41]. It is clear that glial cells under culture conditions exhibit an altered phenotype that can misrepresent certain aspects of their gene expression pattern *in vivo*, including ectopic expression of receptors[42,43]. Note that consistent with our present findings, a large scale RNA sequencing study in neurons and glia[44] and *in situ* hybridization experiments[19] indicated that microglia do not express MOR. We also report that MOR knockout mice show intact morphine-induced microglial activation, but do not develop OIH, indicating a dissociation between OIH and histological indications of microgliosis. The molecular mechanisms underlying the activation of microglia during chronic morphine treatment must therefore occur through a receptor other than MOR. Several alternate pathways for microglial activation underscore the complexity of the processes triggering microgliosis, highlighting the possibility that molecules released from neurons, in addition to or instead of direct action of morphine on microglia, might be responsible for the activation response observed following morphine treatment (Figure 1c,d). For example, the pattern recognition receptor toll-like receptor 4 (TLR4) on microglia may trigger their activation by binding damage associated molecular patterns (DAMPs) released from neurons or through binding morphine itself, however this last point remains controversial[10,19]. Recent studies rather suggest that TLR4 is not required for microglial activation by morphine[21], or for opioid tolerance and hyperalgesia[20]. Other proposed key mediators controlling microglial activation states include TLR2[45], the microglial ATP receptor P2X4[41], and CSF1R[46]. Thus, we propose that opioid action at MOR expressed by nociceptors, and not by microglia, initiates downstream events in pain pathways (e.g. in spinal, brain, and descending circuits), which in turn could contribute to the molecular, synaptic, and network-level adaptations that result in tolerance and OIH, as well as microglial activation and LTP[47].

Opioid-induced spinal LTP at nociceptor synapses[28,36] is now considered to be an essential contributor to OIH, and may also contribute to tolerance. However, the mechanisms underlying opioid-induced spinal LTP remain disputed, in particular the pre-[28,37] versus post-[27] synaptic initiating events. At present, our optogenetic interrogation of synaptic transmission between TRPV1 nociceptors and dorsal horn neurons reveals that the deletion of presynaptic MOR not only eliminates DAMGO-induced depression of neurotransmission, but also abolishes LTP, supporting the presynaptic origin hypothesis. We therefore propose that prolonged activation of MOR in nociceptors has predominantly pro-nociceptive effects during chronic opioid exposure[23,36], and initiates downstream plasticity throughout nociceptive circuits in the central nervous system to drive the development of tolerance and OIH[12]. At this time, we cannot make definitive conclusions regarding the cellular localization of MOR that contribute to tolerance and OIH within nociceptors (i.e. MOR at the peripheral nerve terminals in the skin, along the nociceptor axons, or at the nociceptor cell body). Note, however, that repeated intradermal administration of MOR agonists[23], which arguably only act on MOR at nociceptor peripheral terminals, or chronic administration of the peripherally acting opioid loperamide[48] is sufficient to induce OIH and/or antinociceptive tolerance.

While opioids remain widely used in the treatment of perioperative, cancer, and chronic non-cancer pain, recent re-evaluation of their side effect profile has highlighted dose escalation as a direct contributor to increased morbidity and mortality[4,49]. Risk mitigation strategies that have the potential to decrease opioid tolerance and OIH, and therefore limit dose escalation, are urgently needed to help stem the current Opioid Epidemic. Based on our results with MOR cKO mice and MNB in uninjured mice and mice with perioperative and chronic pain, we propose that tolerance in humans might be improved by blocking MOR in nociceptors. Peripherally restricted opioid antagonists, such as MNB and oral naloxone, are clinically available as treatments for opioid-induced constipation in non-cancer patients. Clinical trials have found no or minimal increases in pain or withdrawal symptoms after administration of these drugs[50,51]. To date, no clinical studies have directly assessed the utility of peripheral MOR antagonists to reduce opioid analgesic tolerance. However, a recent Phase III report on MNB for opioid-induced constipation found that, compared to placebo-treated patients on a routine morphine schedule, patients taking MNB (12 mg once every other day) had stable or decreased morphine use after 1 – 4 weeks, with no increases in visual analogue scale (VAS) pain scores[52]. In addition, the effects of orally administered prolonged-release oxycodone/naloxone combination on pain relief and opioid-induced constipation in patients with chronic pain resulted in significant reductions in pain scores, compared to treatment with oxycodone alone[53]. Given that the opioid antagonist naloxone has very low oral bioavailability and extensive first pass metabolism, these results suggest that its effect, in this context, is through blockade of peripheral opioid receptors. In contrast, one clinical study reported that MNB administration increased morphine consumption in patients within the first 4 hours after surgery, but not later[54]. The particularly high dose of MNB (0.9 mg/kg) used, i.e. 6-fold higher than the current recommended therapeutic dose, and twice higher than a dose previously shown to have CNS effects[55], might have resulted in blockade of CNS sites as peripheral restriction of MNB is known to be dose-dependent[56]. Consistent with this possibility, patients administered a high dose of MNB, but not placebo, showed a higher incidence of nausea and vomiting[54], indicating a withdrawal syndrome from blockade of central MOR that could explain the increased morphine consumption. Importantly, this finding, along with preclinical studies using peripheral MOR antagonists, suggest that peripheral MOR signaling contributes to endogenous analgesia within hours of an injury[57], whereas central MOR signaling mediates considerable endogenous analgesia over longer periods, from days to months after injury[58]. Indeed, we did not find that MNB increased pain associated with orthotrauma or nerve damage, indicating that endogenous analgesia mechanisms are unaffected by this treatment.

We conclude that MOR expressed on primary afferent nociceptors drive the initiation of adverse counter-adaptations to opioids responsible for the onset of analgesic tolerance and OIH. Our data support the development of therapeutic strategies for disrupting peripheral MOR signaling in order to maintain adequate long-lasting pain control while limiting potentially harmful opioid dose escalation. The design of human trials aimed at rigorously evaluating the translational potential of opioid agonist/peripheral opioid antagonist combinations in appropriate patients with opioid-responsive pain conditions will be essential to the development of safer and more effective pain management strategies.

ONLINE METHODS

Animals

All procedures were approved by the Stanford University Administrative Panel on Laboratory Animal Care in accordance with American Veterinary Medical Association guidelines and the International Association for the Study of Pain. Mice were housed 2–5 per cage and maintained on a 12-hour light/dark cycle in a temperature-controlled environment with *ad libitum* access to food and water.

To specifically ablate the MOR in primary afferent nociceptors (MOR cKO), mice bearing a conditional allele of the *Oprm1* gene containing loxP sites flanking exons 2 and 3 generated previously[59] were crossed with transgenic mice expressing Cre under the control of the TRPV1 gene promoter, B6.129-Trpv1tm1(Cre)Bbm/J (TrpV1-cre, purchased from the Jackson Laboratory). Deletion of the *Oprm1* exons 2 and 3 results in a frameshift that disrupts MOR function in MOR cKO mice. MOR cKO mice were born in the expected Mendelian ratios and showed no gross anatomical or behavioral defects, similar to the global MOR knockout mouse[8]. To confirm selective ablation of MOR in the DRG only of MOR cKO mice, we performed PCR on genomic DNA from DRG, spinal cord and brain using the following primers for the excised band forward primer (5'-ACCAGTACATGGACTGGATGTGCC-3') and reverse primer (5'-GAGACAAGGCTCTGAGGATAGTAA -3') which resulted in a 363 bp DNA fragment that was seen in DRG but absent in spinal cord and brain (Supplemental Figure 3). Control subjects were littermate mice without the $Oprm1^{flox/flox}$ alleles: $Trpv1^{Cre}$; $Oprm1^{+/+}$. For MOR cKO behavioral and electrophysiological studies, we used male and female mice (8 – 15 and 6 – 8 weeks, respectively). For all other experiments, we used male C57Bl6/J mice (8 – 15 weeks). Based on a power analysis, assuming 10–20% behavioral variability as in our previous work[23], 8–12 mice per genotype is sufficient for each experimental group to reliably detect a 25% difference in means between genotypes.

Drugs and Routes of Administration

Drugs—Morphine sulfate (1 μg, intrathecal; 10 – 40 mg/kg/b.w., subcutaneous, West-Ward NDC 0641-6070-01, Lot# 114342), methylnaltrexone bromide (0.1 – 10 mg/kg/b.w., subcutaneous, Salix Pharmaceuticals Inc. NDC 65649-551-07 [data in Figure 4 and Supplemental Figures 13, 15, 16], and Sigma SML0277 [data in Supplemental Figure 14]). Drug vehicle and dilutions used 0.9% sodium chloride (Hospira NDC 0409-4888-10, Lot# 35-243-DK).

Subcutaneous injection—In lightly restrained, unanesthetized mice a 30 G needle attached to a microsyringe was inserted through the skin and the drug (200–250 μl volume) is injected into the subcutaneous space.

Intrathecal injection—In lightly-restrained, unanesthetized mice, a 30 G needle attached to a microsyringe was inserted between the L4/L5 vertebrae, puncturing through the dura (confirmation by presence of reflexive tail flick), followed by injection of 2 – 5 μl as previously described[58].

Behavioral testing

For consistency, one experimenter (G.C.) performed all *in vivo* drug administrations and behavioral testing with the exception of data in Figure 5a–e (G.C. and J.R.D.). All testing was conducted between 10:00 am – 3:00 pm in an isolated, temperature- and light-controlled room. Mice were acclimated for 30 – 60 min in the testing environment within custom red plastic cylinders (4" D) on a raised metal mesh platform (24" H). The male experimenter's lab coat was present in the testing room for the first 30 minutes of acclimation, and then the experimenter entered the room for the final 30 minutes before commencement of testing to eliminate potential olfactory-induced changes in nociception[60]. The experimenter was blind to treatment and/or genotype throughout: all drugs were given to the experimenter in coded vials, and decoded only upon completion of testing. Mice of different genotypes were placed in randomized and coded holding cylinders for all sensory testing by V.L.T. or D.W., and only after testing was G.C. unblinded. Mice were randomized by simple selection from their homecage (5 mice per cage) prior to testing, and assigned a number. For daily testing, a secondary experimenter (V.L.T.) changed the order of the mice to be tested; the primary experimenter (G.C.) was blind to this order. Mice were only excluded from the study if they were found to have extensive bodily wounds from aggressions with cage mates, as the presence of additional injuries introduces potential confounds, such as alterations to the endogenous opioid system[58].

Classification of mouse behaviors into reflexive and affective-motivational nociceptive responses—To rigorously define the appearance of pain-like and pain-relief-like behaviors in non-verbal animals, we have adopted a strict taxonomy, as recommended by the International Association for the Study of Pain (IASP), so as not to over-extend or inappropriately anthropomorphize rodent behaviors[61]. For example, we limit our description of pain-like behavior in mice to the use of words such as "nociceptive", "antinociceptive", "hypersensitivity", "nociception-induced affective-motivational behavior", etc., and reserve words such as "pain", "hyperalgesia", "analgesia", etc. to descriptions of the human experience and the clinical effects of opioids. In mice, a cutaneous noxious stimulus can elicit several distinct behavioral responses[62]: 1. Withdrawal reflexes: rapid reflexive retraction or digit splaying of the paw that occur in response to nociceptive sensory information, but cease once the stimulus is removed and afferent nociceptive information stops; 2. Affective-motivational responses: temporally-delayed (relative to the noxious stimulus contact or removal of said stimulus), directed licking and biting of the paw (termed "attending"), extended lifting or guarding of the paw, and/or escape responses characterized by hyperlocomotion, rearing or jumping away from the noxious stimulus. Paw withdrawal reflexes are classically measured in studies of hypersensitivity, and involve spinal cord and brainstem circuits (as these behaviors are observed in decerebrate rodents only whilst the stimulus is in contact with tissue, but immediately cease once the stimulus is removed[63]). In contrast, affective-motivational responses are complex behaviors requiring processing by limbic and cortical circuits in the brain, the appearance of which indicates the subject's motivation and arousal to make the aversive sensations cease, by licking the affected tissue, protecting the tissue, or seeking an escape route[63–69].

Mechanical nociception assays—To evaluate mechanical reflexive hypersensitivity[58], we used a logarithmically increasing set of 8 von Frey filaments (Stoelting), ranging in gram force from 0.007 to 6.0 g. These were applied perpendicular to the plantar hindpaw with sufficient force to cause a slight bending of the filament. A positive response was characterized as a rapid withdrawal of the paw away from the stimulus filament within 4 s. Using the up-down statistical method[70], the 50% withdrawal mechanical threshold scores were calculated for each mouse and then averaged across the experimental groups.

To evaluate mechanical-induced affective-motivational responses we used three von Frey filaments (0.07 g, 0.4 g, and 2.0 g). Each filament was applied for one second to the hindpaw, and the duration of attending behavior was collected for up to 30 seconds after the stimulation. Only one stimulation per filament was applied on a given testing session, in order to prevent behavioral sensitization that can result from multiple noxious stimulations and then averaging those responses.

Thermal nociception assays—To evaluate thermal reflexive hypersensitivity[62], we used the tail-immersion test (temperature of the water bath was set to 48 – 52.5 °C, as indicated in the text or figures). The mouse was gently restrained and 2 cm of the tip of the tail was submerged in the water bath, and the latency (seconds) to reflexively withdraw the tail from the water was recorded as a positive nociceptive reflex response. A maximal cut-off of 45 – 60 s was set to prevent tissue damage. Only one tail immersion was applied on a given testing session, in order to prevent behavioral sensitization that can result from multiple noxious immersions and then averaging those responses.

To evaluate thermal-induced affective-motivational responses[62], we used the hotplate test (plate temperature was set to 50 – 52.5 °C). Mice were place on the plate and the latency (seconds) to the first appearance of an attending response (lick and/or bite at one or both hindpaws) was recorded as a positive affective-motivational response. A maximal cut-off of 45 s was set to prevent tissue damage. Only one exposure to the hotplate was applied on a given testing session, in order to prevent behavioral sensitization that can result from multiple noxious exposures and then averaging those responses.

To evaluate affective-motivational responses to an acute, focal thermal stimulus[71], we applied either a single, unilateral 50 μl drop of 55 °C water or acetone (evaporative cooling) to the left hindpaw, and the duration of attending behavior was collected for up to 30 seconds after the stimulation. Only one stimulation per thermal drop was applied on a given testing session, in order to prevent behavioral sensitization that can result from multiple noxious stimulations and then averaging those responses.

To evaluate affective-motivational responses to a sustained, inescapable noxious thermal stimulus mice were placed on a 52.5 °C hot plate for 45 seconds. A high-speed camera (on the side, level with the hot plate floor) was used to capture the movement, speed, velocity, and detailed reflexive and affective-motivational behaviors of the mice, as described above. As opposed to the standard hot plate test, we scored all behaviors such as reflexive paw flinching (rapid flicking of the limb), paw attending (directed licking of the limb), paw guarding (intentional lift protection of the limb), and escape jumping for the duration of the

trial. This allows us to analyze the high-speed videos, blinded to plate temperature or treatment, for the total time spent engaging in affective-motivational behaviors and the number of nociceptive reflexives, as opposed to the traditional metric of merely determining the latency to the first reflexive response. The time the animal spends engaging in these affective-motivational behaviors reflects the degree to which the animal translates nociceptive information into an aversive signal that instructs the animal to initiate behaviors that will lessen the aversive qualities of the on-going nociceptive information (i.e. licking the tissue, and protecting the tissue by guarding or seeking escape). To evaluate the presence of chronic morphine antinociceptive tolerance, mice are subjected to this modified hotplate assay on both the first day of morphine treatment and again on the last day of chronic morphine dosing.

Spinal cord slice preparation and electrophysiology

Adult mice (6 – 8 weeks old) were anesthetized with isoflurane, decapitated, and the vertebral column was rapidly removed and placed in oxygenated ice-cold dissection solution (in mM: 95 NaCl, 2.5 KCl, 1.25 NaH2PO4, 26 NaHCO3, 50 sucrose, 25 glucose, 6 MgCl2, 1.5 CaCl2, and 1 kynurenic acid, pH 7.4, 320 mOsm). The lumbar spinal cord was isolated, embedded in a 3% agarose block, and transverse slices (400 μm thick) were made using a vibrating microtome (Leica VT 1200S). Slices were incubated in oxygenated recovery solution (in mM: 125 NaCl, 2.5 KCl, 1.25 NaH2PO4, 26 NaHCO3, 25 glucose, 6 MgCl2, and 1.5 CaCl2, pH 7.4, 320 mOsm) at 35°C for 1 hour before recording. Patch-clamp recording in whole-cell configuration was performed at 32°C on lamina I or lamina II outer zone neurons visualized with an Olympus microscope (BX51WI age-MTI). Slices were perfused at ~2 ml/min with recording solution (in mM: 125 NaCl, 2.5KCl, 1.25 NaH2PO4, 26 NaHCO3, 25 glucose, 1 MgCl2, 2 CaCl2, pH 7.4, 320 mOsm). Recordings were performed in voltage-clamp mode at a holding potential of −70 mV. Thick-walled borosilicate pipettes, having a resistance of 3–6 MOhm, were filled with internal solution (in mM: 120 potassium gluconate, 20 KCl, 2 MgCl2, 5 MgATP, 0.5 NaGTP, 20 HEPES, 0.5 EGTA, PH 7.25 with KOH, ~300 mOsm). All data were acquired using a Multiclamp 700B amplifier and pClamp10 software (Molecular Devices). Sampling rate was 10 kHz and data were filtered at 2 kHz. Analysis of eEPSC peak amplitudes was done with Clampfit software (pClamp10, Molecular Devices). Graphs and statistical analysis were generated with Igor Pro (Wave Metrics).

Optogenetic stimulation—To isolate the TRPV1 nociceptor mediated EPSCs, we crossed the TRPV1-Cre mice with Ai32 mice (Rosa-CAG-LSL-ChR2(H134R)-EYFP-WPRE)[72] to limit the channelrhodopsin 2 expression specifically to TRPV1 primary afferents. The TRPV1 nociceptor mediated EPSCs were evoked by blue light (0.2 ms, 0.03 HZ) generated by an LED Transmitted Light Source (Lambda TLED, Sutter). For all recordings, 10 μm bicuculline and 2 μm strychnine were included in the recording solution to eliminate the contribution of γ-aminobutyric acid type A (GABAA) or glycine receptors on the C-fiber or TRPV1 afferent mediated EPSC.

Immunohistochemistry

Mice (8 – 10 weeks) were transcardially perfused with 10% formalin in PBS. The brains, DRG (L3–L5), and spinal cord (lumbar cord L3 – L5 segments) were dissected from the mice and cryoprotected in 30% sucrose in PBS. Tissues were then frozen in O.C.T. (Sakura Finetek, Inc.). Tissue sections (30 m for the brains; 40 μm for spinal cord; and 10 μm for DRG) were prepared using a cryostat (Leica Biosystems) and blocked with PBS containing 5% normal donkey serum and 0.3% Triton X-100 for 1 h at room temperature. The sections were then incubated with primary antibodies, indicated in each figure, at 4 °C, overnight. For the chicken anti-GFP antibody, the incubation was performed at 37 °C for 2 h. After extensive wash with PBS containing 1% normal donkey serum and 0.3% Triton X-100, sections were incubated with appropriate secondary antibody conjugated to AlexaFluor for 2 h at room temperature. Images were collected under a Leica TCS SP5II confocal microscope with LAS AF Lite software (Leica Microsystems).

The following primary antibodies were used: anti-CD11b, Abd Serotec # MCA711G (rat, 1:1,000), anti-CGRP: Abcam ab22560 (sheep; 1:2000); anti-GFP: Molecular Probes (rabbit; 1:1000), anti-TRPV1: gift from David Julius, UCSF (guinea-pig; 1:10000); anti-MOR used in Figure 1: Abcam 134054 (rabbit; 1:100), anti-MOR used in Figure 2: gift from Chris Evans, UCLA (rabbit; 1:300); anti-MOR used in Figure 1: Abcam 10275 (rabbit; 1:100); anti-MOR: Neuromics GP10106 (guinea pig, 1:1,000). To identify IB4-binding cells, biotinylated IB4 Sigma L2140 (1:500) and fluorophore-conjugated streptavidin (Molecular Probes, 1:1000) were used in place of primary and secondary antibodies.

In situ hybridization

In situ hybridization (ISH) was performed using the Panomics QuantiGene ViewRNA tissue assay (Affymetrix/Panomics), as previously described[73]. The probe set provided by Affymetrix for hybridization to the mouse mu opioid receptor (*Oprm1*) coding region (NM_001039652) consists of 9 blocking probes and 40 short (15–25 base pair) oligonucleotide primers upon which a branched DNA amplification “tree” is built. This methodology provides single copy sensitivity and 8,000-fold signal amplification of each target mRNA through a unique branching amplification. The signal was detected by an alkaline phosphatase reaction with the Fast Red substrate, which was visualized by bright field or fluorescent microscopy. In order to combine *Oprm1* ISH with immunohistochemistry for microglial marker CD11b, the following protocol was developed: C57BL/6J wild-type mice were deeply anesthetized with isoflurane and transcardially perfused with 0.1M PBS followed by 10% formalin in PB. Lumbar DRGs were dissected, cryoprotected in 30% sucrose overnight and then frozen in OCT. Tissue was then sectioned at 12–14 μm onto Superfrost Plus slides and kept at −80°C until use. Slides were thawed and then placed directly into 10% formalin for 10 minutes and then subsequently processed according to the manufacturer's protocol. We determined that protease treatment for 12 minutes was optimal and following this, slides were incubated for 3 hours with the RNA probe set at 40°C. After washing, pre-amplifier hybridization and hybridization with an alkaline phosphatase-based method to detect the ISH probe, the slides were blocked in 5% normal donkey serum / 0.1M PBS (without Triton X-100) for one hour at room temperature and then processed for immunohistochemistry as described above.

Microglia RNA library construction and sequencing

Adult (P60) C57BL/6J mice were perfused with ice cold PBS and L4 to L6 lumbar segments of spinal cords were isolated using ribs and vertebra as landmarks. Spinal cords that retained any detectable redness (indicating presence of blood) after perfusion were discarded. Lumbar segments from 4 to 15 mice per group were pooled and mechanically dissociated in HBSS (Gibco) containing 0.5% Glucose, 15 mM HEPES pH 7.5, and 125 U/mL DNaseI (Sigma). Dissociated tissue was subjected to MACS myelin removal (Myelin Removal Beads II, Miltenyi) followed by CD11b selection (CD11b Microbeads, Miltenyi) according to the manufacturer's instructions, except all centrifugation steps were shortened to 30 s at 10,000 rcf. The isolation was performed rapidly (less than 3 hours) and care was taken to keep the cells chilled throughout to minimize gene expression changes caused by the procedure.

Total RNA was extracted from CD11b-positive cells using the RNeasy Plus Micro Kit (Qiagen). For each replicate, 10 ng of high quality total RNA (RIN > 9.0) was used to prepare a poly-A enriched cDNA library using the SMARTer Ultra Low Input RNA Kit for Sequencing - v3 (Clontech). Supplemental morphine and saline treatment RNA libraries were prepared with Smart-Seq2[74]. Libraries were modified for sequencing using the Nextera XT DNA Sample Preparation Kit (Illumina) with 300 pg of cDNA as input material. Libraries were sequenced using the Illumina Nextseq to obtain 75 bp paired-end reads. Two libraries for each condition were prepared and sequenced independently for an average of 15.7 million reads per group.

Sequencing reads were mapped to the UCSC mouse reference genome mm10 essentially as previously described[44]. Mapping was accomplished by using HISAT[75] version 2.0.3 via the Galaxy platform (http://usegalaxy.org), resulting in a minimum 70% concordant pair alignment rate. Wiggle plots were generated using BEDTools[76] and BedGraph-to-bigWig converter in Galaxy and the UCSC genome browser. Transcript FPKM (fragments per kilobase of transcript sequence per million mapped fragments) values were obtained using Cufflinks[77] version 2.2.1 with the iGenomes mm10 reference annotation.

Pain models

Neuropathic pain—Two bilateral peripheral nerve injuries were performed: chronic constriction injury (CCI) (Bennet and Xie, 1988) and complete transection of the sciatic nerve (Wall et al., 1979). Briefly, adult C57BL6J mice were anesthetized with isoflurane, and one sciatic nerve at a time was exposed at mid-thigh level. For CCI, two 5-0 silk sutures were loosely tied around the nerve about 2 mm apart. In the complete transection model, a 2 mm portion of the nerve was excised. The wound was closed with tissue adhesive (Vetbond) and the procedure was repeated on the other side. Two or seven days after injury spinal cords were collected for RNAseq as described above. For behavior, injuries were performed unilaterally and mice were tested beginning seven days after the surgery.

Orthotrauma inflammatory pain—Mice were anesthetized with isoflurane and underwent a distal tibia fracture and an intramedullary pin fixation in the right leg, as previously described[78]. Briefly, to make the shaft for the bone pinning, a small hole was

made in the proximal tibia and a 27 G needle was inserted down the medullary axis of the bone, and then removed. Next, the distal tibia was scored with a bone saw and fractured. To set the fracture, the 27 G needle was re-inserted into the intramedullary space, through the proximal tibia, and advanced across the fracture site to the distal portion of bone. The wound was closed with sterile staples. For behavior, mice were tested beginning seven days after the surgery.

Data and statistical analyses

All experiments were randomized and performed by a blinded researcher. Researchers remained blinded throughout histological, biochemical, and behavioral assessments. Groups were unblinded at the end of each experiment before statistical analysis. Data are expressed as the mean ± s.e.m. Data were analyzed using a Kruskal-Wallis or Student's t tests, or ordinary or repeated measures one-way or two-way ANOVA, with a Bonferroni posthoc test, as indicated in the main text or figure captions, as appropriate. For dose-response hyperalgesia studies the best-fit line was generated following non-linear regression analysis based on the % Maximum Possible Effect (MPE) for each mouse; calculated as: MPE = [(drug induced threshold – basal threshold) / basal threshold] X 100.

Supplementary Material

Refer to Web version on PubMed Central for supplementary material.

Acknowledgments

This work was supported by National Institutes of Health (NIH) Grant DA031777 (G.S.), the Rita Allen Foundation and American Pain Society Award in Pain (G.S.), NIH Postdoctoral NRSA F32DA041029 (G.C.), Foundation for Anesthesia Education and Research (FAER) Mentored Research Training Grant (V.L.T.), NIH Postdoctoral Fellowship T32GM089626 (D.W.), DoD National Defense Science & Engineering Graduate (NDSEG) Fellowship (E.I.S.), NSF Graduate Research Fellowship and Stanford Bio-X Graduate Fellowship (J.R.D.), NIH Grant R37DA15043 (B.A.B.), and Damon Runyon Cancer Research Foundation postdoctoral fellowship (C.J.B.). We thank Brigitte Kieffer (McGill University) for providing the Oprm1 floxed mice and fluorescent reporter MOR-mCherry mice, Chris Evans (University of California, Los Angeles) and Frédéric Simonin (Universite´de Strasbourg) for providing critical immunohistochemical and pharmacological reagents, Jonathan Kaslow and Andy Yu-Chun Wong for assistance with data analysis, and Huy Nguyen (Stanford University) for assistance with illustration design.

REFERENCES

1. Carroll IR, Angst MS, Clark JD. Management of perioperative pain in patients chronically consuming opioids. Reg. Anesth. Pain Med. 2004; 29:576–591. [PubMed: 15635517]
2. Kalso E, Edwards JE, Moore RA, McQuay HJ. Opioids in chronic non-cancer pain: Systematic review of efficacy and safety. Pain. 2004; 112:372–380. [PubMed: 15561393]
3. A. Pizzo P, M. Clark N, Carter Pokras O. Relieving Pain in America: A Blueprint for Transforming Prevention, Care, Education, and Research. Institute of Medicin. 2011
4. Volkow N, McLellan T. Opioid Abuse in Chronic Pain — Misconceptions and Mitigation Strategies. N. Engl. J. Med. 2016; 374
5. Chu LF, Angst MS, Clark D. Opioid-induced hyperalgesia in humans: molecular mechanisms and clinical considerations. Clin. J. Pain. 2008; 24:479–496. [PubMed: 18574358]
6. Angst M, Clark JD. Opioid-induced Hyperalgesia: A Qualitative Systematic Review. Anesthesiology. 2006; 104:570–587. [PubMed: 16508405]
7. Collett BJ. Opioid tolerance: the clinical perspective. Br. J. Anaesth. 1998; 81:58–68. [PubMed: 9771273]

8. Matthes HW, et al. Loss of morphine-induced analgesia, reward effect and withdrawal symptoms in mice lacking the mu-opioid-receptor gene. Nature. 1996; 383:819–823. [PubMed: 8893006]
9. Mansour A, Fox Ca, Akil H, Watson SJ. Opioid-receptor mRNA expression in the rat CNS: anatomical and functional implications. Trends Neurosci. 1995; 18:22–29. [PubMed: 7535487]
10. Ferrini F, Trang T, Mattioli T. Morphine hyperalgesia gated through microglia-mediated disruption of neuronal Cl-homeostasis. Nat. Neurosci. 2013; 16:183–192. [PubMed: 23292683]
11. Wang Y, et al. Blockade of PDGFR-β activation eliminates morphine analgesic tolerance. Nat. Med. 2012; 18:385–387. [PubMed: 22344297]
12. Christie MJ. Cellular neuroadaptations to chronic opioids: tolerance, withdrawal and addiction. Br. J. Pharmacol. 2008; 154:384–396. [PubMed: 18414400]
13. Rivat C, Ballantyne J. The dark side of opioids in pain management : basic science explains clinical observation. 2016; 1:1–9.
14. Roeckel L-A, Le Coz G-M, Gaveriaux-Ruff C, Simonin F. Opioid-induced Hyperalgesia: Cellular and Molecular Mechanisms. Neuroscience. 2016
15. Trang T, et al. Pain and Poppies: The Good, the Bad, the Ugly of Opioid Analgesics. J. Neurosci. 2015; 35:13879–13888. [PubMed: 26468188]
16. Raghavendra V, Tanga FY, DeLeo JA. Attenuation of Morphine Tolerance, Withdrawal-Induced Hyperalgesia, and Associated Spinal Inflammatory Immune Responses by Propentofylline in Rats. Neuropsychopharmacology. 2004; 29:327–334. [PubMed: 14532913]
17. Watkins LR, Hutchinson MR, Rice KC, Maier SF. The 'Toll' of Opioid-Induced Glial Activation: Improving the Clinical Efficacy of Opioids by Targeting Glia. Trends Pharmacol. Sci. 2009; 30:581–591. [PubMed: 19762094]
18. Kao S-C, et al. Absence of μ opioid receptor mRNA expression in astrocytes and microglia of rat spinal cord. Neuroreport. 2012; 23:378–384. [PubMed: 22362187]
19. Hutchinson MR, et al. Evidence that opioids may have toll-like receptor 4 and MD-2 effects. Brain. Behav. Immun. 2010; 24:83–95. [PubMed: 19679181]
20. Mattioli TA, et al. Toll-like receptor 4 mutant and null mice retain morphine-induced tolerance, hyperalgesia, and physical dependence. PLoS One. 2014; 9:1–14.
21. Fukagawa H, Koyama T, Kakuyama M, Fukuda K. Microglial activation involved in morphine tolerance is not mediated by toll-like receptor 4. J. Anesth. 2013; 27:93–97. [PubMed: 22926420]
22. Mao J. Opioid-induced abnormal pain sensitivity: Implications in clinical opioid therapy. Pain. 2002; 100:213–217. [PubMed: 12467992]
23. Joseph EK, Reichling DB, Levine JD. Shared mechanisms for opioid tolerance and a transition to chronic pain. J Neurosci. 2010; 30:4660–4666. [PubMed: 20357116]
24. Ruscheweyh R, Wilder-Smith O, Drdla R, Liu X-G, Sandkühler J. Long-term potentiation in spinal nociceptive pathways as a novel target for pain therapy. Mol. Pain. 2011; 7:20. [PubMed: 21443797]
25. Reichling DB, Levine JD. Critical role of nociceptor plasticity in chronic pain. Trends Neurosci. 2009; 32:611–618. [PubMed: 19781793]
26. Heinke B, Gingl E, Sandkühler J. Multiple targets of μ-opioid receptor-mediated presynaptic inhibition at primary afferent Aδ- and C-fibers. J. Neurosci. 2011; 31:1313–1322. [PubMed: 21273416]
27. Drdla R, Gassner M, Gingl E, Sandkuhler J. Induction of synaptic long-term potentiation after opioid withdrawal. Science (80-.). 2009; 325:207–210.
28. Zhou H-YY, Chen S-RR, Chen H, Pan H-LL. Opioid-induced long-term potentiation in the spinal cord is a presynaptic event. J Neurosci. 2010; 30:4460–4466. [PubMed: 20335482]
29. Chen SR, Prunean a, Pan HML, Welker KL, Pan HML. Resistance to morphine analgesic tolerance in rats with deleted transient receptor potential vanilloid type 1-expressing sensory neurons. Neuroscience. 2007; 145:676–685. [PubMed: 17239544]
30. Scherrer G, et al. Dissociation of the opioid receptor mechanisms that control mechanical and heat pain. Cell. 2009; 137:1148–1159. [PubMed: 19524516]
31. Usoskin D, et al. Unbiased classification of sensory neuron types by large-scale single-cell RNA sequencing. Nat. Neurosci. 2014; 18:145–153. [PubMed: 25420068]

32. Pasternak GW. Opioids and their receptors: Are we there yet? Neuropharmacology. 2014; 76:198–203. [PubMed: 23624289]
33. Cavanaugh DJ, et al. Restriction of transient receptor potential vanilloid-1 to the peptidergic subset of primary afferent neurons follows its developmental downregulation in nonpeptidergic neurons. J. Neurosci. 2011; 31:10119–10127. [PubMed: 21752988]
34. Kemp T, Spike RC, Watt C, Todd aJ. The mu-opioid receptor (MOR1) is mainly restricted to neurons that do not contain GABA or glycine in the superficial dorsal horn of the rat spinal cord. Neuroscience. 1996; 75:1231–1238. [PubMed: 8938756]
35. Heinke B, Gingl E, Sandkuhler J. Multiple targets of mu-opioid receptor-mediated presynaptic inhibition at primary afferent Adelta- and C-fibers. J Neurosci. 2011; 31:1313–1322. [PubMed: 21273416]
36. Heinl C, Drdla-Schutting R, Xanthos DN, Sandkuhler J. Distinct Mechanisms Underlying Pronociceptive Effects of Opioids. J. Neurosci. 2011; 31:16748–16756. [PubMed: 22090501]
37. Zhao YL, Chen SR, Chen H, Pan HL. Chronic opioid potentiates presynaptic but impairs postsynaptic N-methyl-D-aspartic acid receptor activity in spinal cords: Implications for opioid hyperalgesia and tolerance. J. Biol. Chem. 2012; 287:25073–25085. [PubMed: 22679016]
38. Russell J, Bass P, Goldberg LI, Schuster CR, Merz H. Antagonism of gut, but not central effects of morphine with quaternary narcotic antagonists. Eur. J. Pharmacol. 1982; 78:255–261. [PubMed: 7200037]
39. Stiene-Martin A, Zhou R, Hauser KF. Regional, developmental, and cell cycle-dependent differences in mu, delta, and kappa-opioid receptor expression among cultured mouse astrocytes. Glia. 1998; 22:249–259. [PubMed: 9482211]
40. Turchan-Cholewo J, et al. Cell-specific actions of HIV-Tat and morphine on opioid receptor expression in glia. J. Neurosci. Res. 2008; 86:2100–2110. [PubMed: 18338799]
41. Horvath RJ, Romero-Sandoval EA, Leo J. a De. Inhibition of microglial P2X4 receptors attenuates morphine tolerance, Iba1, GFAP and ?? opioid receptor protein expression while enhancing perivascular microglial ED2. Pain. 2010; 150:401–413. [PubMed: 20573450]
42. Caldeira C, et al. Microglia change from a reactive to an age-like phenotype with the time in culture. Front. Cell. Neurosci. 2014; 8:1–16. [PubMed: 24478626]
43. Foo LC, et al. Development of a method for the purification and culture of rodent astrocytes. Neuron. 2011; 71:799–811. [PubMed: 21903074]
44. Zhang Y, et al. An RNA-Sequencing Transcriptome and Splicing Database of Glia, Neurons, and Vascular Cells of the Cerebral Cortex. 2014; 34:1–19.
45. Zhang Y, et al. Essential role of toll-like receptor 2 in morphine-induced microglia activation in mice. Neurosci. Lett. 2011; 489:43–47. [PubMed: 21130144]
46. Guan Z, et al. Injured sensory neuron–derived CSF1 induces microglial proliferation and DAP12-dependent pain. Nat. Neurosci. 2015; 19:1–10.
47. Kronschläger MT, et al. Gliogenic LTP spreads widely in nociceptive pathways. Science (80-.). 2016; 5715
48. He SQ, et al. Tolerance develops to the antiallodynic effects of the peripherally acting opioid loperamide hydrochloride in nerve-injured rats. Pain. 2013; 154:2477–2486. [PubMed: 23880055]
49. Chen, LH., Hedegaard, H., Warner, M. Drug-poisoning Deaths Involving Opioid Analgesics: United States, 1999–2011; NCHS Data Brief. 2014. p. 1-8.at<http://www.ncbi.nlm.nih.gov/pubmed/25228059>
50. Thomas J, et al. Methylnaltrexone for opioid-induced constipation in advanced illness. N. Engl. J. Med. 2008; 358:2332–2343. [PubMed: 18509120]
51. Yu CS, et al. Safety and efficacy of methylnaltrexone in shortening the duration of postoperative ileus following segmental colectomy: Results of two randomized, placebo-controlled phase 3 trials. Dis. Colon Rectum. 2011; 54:570–578. [PubMed: 21471758]
52. Webster LR, et al. Analysis of opioid-mediated analgesia in phase III studies of methylnaltrexone for opioid-induced constipation in patients with chronic noncancer pain. J. Pain. Res. 2015; 8:771–780. [PubMed: 26586963]
53. Poelaert J, et al. Treatment with prolonged-release oxycodone/naloxone improves pain relief and opioid-induced constipation compared with prolonged-release oxycodone in patients with chronic

severe pain and laxative-refractory constipation. Clin. Ther. 2015; 37:784–792. [PubMed: 25757607]

54. Jagla C, Martus P, Stein C. Peripheral opioid receptor blockade increases postoperative morphine demands—A randomized, double-blind, placebo-controlled trial. Pain. 2014; 155:2056–2062. [PubMed: 25046272]
55. Zacny JP, Wroblewski K, Coalson DW. Methylnaltrexone: its pharmacological effects alone and effects on morphine in healthy volunteers. Psychopharmacology (Berl). 2015; 232:63–73. [PubMed: 24871705]
56. Rosow CE, et al. Reversal of opioid-induced bladder dysfunction by intravenous naloxone and methylnaltrexone. Clin. Pharmacol. Ther. 2007; 82:48–53. [PubMed: 17392726]
57. Stein C, et al. Peripheral mechanisms of pain and analgesia. Brain Res. Rev. 2009; 60:90–113. [PubMed: 19150465]
58. Corder G, et al. Constitutive μ-opioid receptor activity leads to long-term endogenous analgesia and dependence. Science (80-.). 2013; 341:1394–1399.

METHODS-ONLY REFERENCES

59. Weibel R, et al. Mu Opioid Receptors on Primary Afferent Nav1.8 Neurons Contribute to Opiate-Induced Analgesia: Insight from Conditional Knockout Mice. PLoS One. 2013; 8:1–18.
60. Sorge RE, et al. Olfactory exposure to males, including men, causes stress and related analgesia in rodents. Nat. Methods. 2014; 11:629–632. [PubMed: 24776635]
61. Mogil JS. Animal models of pain: progress and challenges. Nat. Rev. Neurosci. 2009; 10:283–294. [PubMed: 19259101]
62. Manglik A, et al. Structure-based discovery of opioid analgesics with reduced side effects. Nature. 2016:1–6.
63. Woolf CJ. Long term alterations in the excitability of the flexion reflex produced by peripheral tissue injury in the chronic decerebrate rat. Pain. 1984; 18:325–343. [PubMed: 6728499]
64. Rescola R. Pavlovian conditioned fear in Sidman avoidance learning. J Comp Physiol Psychol. 1968; 65:55–60. [PubMed: 5648465]
65. Blanchard R, Blanchard D. Passive and active reactions to fear-eliciting stimuli. J Comp Physiol Psychol. 1969; 68:129–135. [PubMed: 5793861]
66. Bolles R. Species-specific defense reactions and avoidance learning. Psychol Rev. 1970; 77:32–48.
67. Bolles R, Fanselow M. A perceptual-defensive-recuperative model of fear and pain. Behav Brain Sci. 1980; 3:291–323.
68. Fanselow MS. The postshock activity burst. Anim. Learn. Behav. 1982; 10:448–454.
69. Darwin, C. The expression of the emotions in man and animals. Albemarle: 1872.
70. Chaplan SR, Bach FW, Pogrel JW, Chung JM, Yaksh TL. Quantitative assessment of tactile allodynia in the rat paw. J. Neurosci. Methods. 1994; 53:55–63. [PubMed: 7990513]
71. Solway B, Bose SC, Corder G, Donahue RR, Taylor BK. Tonic inhibition of chronic pain by neuropeptide Y. Proc. Natl. Acad. Sci. U. S. A. 2011; 108:7224–7229. [PubMed: 21482764]
72. Madisen L, et al. A toolbox of Cre-dependent optogenetic transgenic mice for light-induced activation and silencing. Nat. Neurosci. 2012; 15:793–802. [PubMed: 22446880]
73. Bardoni R, et al. Delta opioid receptors presynaptically regulate cutaneous mechanosensory neuron input to the spinal cord dorsal horn. Neuron. 2014; 81:1312–1327. [PubMed: 24583022]
74. Picelli S, et al. Smart-seq2 for sensitive full-length transcriptome profiling in single cells. Nat. Methods. 2013; 10:1096–1098. [PubMed: 24056875]
75. Kim D, Langmead B, Salzberg SL. HISAT: a fast spliced aligner with low memory requirements. Nat. Methods. 2015; 12:357–360. [PubMed: 25751142]
76. Quinlan AR, Hall IM. BEDTools: A flexible suite of utilities for comparing genomic features. Bioinformatics. 2010; 26:841–842. [PubMed: 20110278]
77. Trapnell C, et al. Transcript assembly and quantification by RNA-Seq reveals unannotated transcripts and isoform switching during cell differentiation. Nat. Biotechnol. 2010; 28:511–515. [PubMed: 20436464]

78. Terrando N, et al. Stimulation of the α7 nicotinic acetylcholine receptor protects against neuroinflammation after tibia fracture and endotoxemia in mice. Mol. Med. 2015; 20:667–675. [PubMed: 25365546]

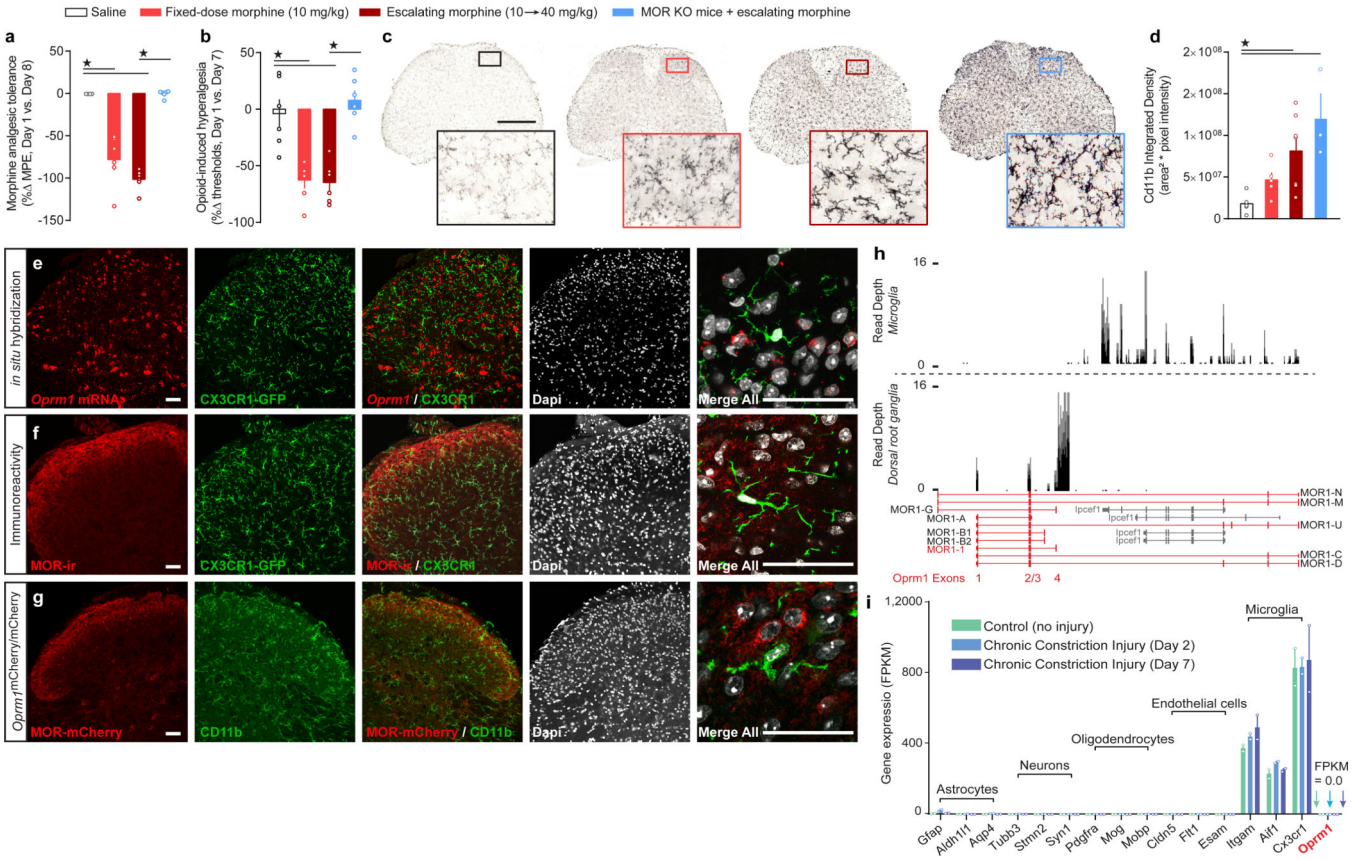

Figure 1. MOR is required for morphine antinociceptive tolerance and OIH, but is not expressed by spinal microglia

(**a–b**) Behavioral indices of chronic morphine side effects: (a) analgesic tolerance ($F_{3, 20}$ = 61.26, $P < 0.0001$) and (b) OIH ($F_{3, 20}$ = 16.96, $P < 0.0001$) in control and MOR KO mice (n = 6 mice for all groups). (**c,d**) Densitometry analysis of anti-CD11b immunoreactivity in spinal cord dorsal horn to assess microglial activation in control and MOR KO mice (P = 0.0032). Scale bar = 500 μm. **(e)** *in situ* hybridization for *Oprm1* mRNA in CX3CR1-eGFP mouse spinal cord. **(f)** Immunohistochemistry for MOR protein in CX3CR1-eGFP mouse spinal cord. **(g)** MOR-mCherry reporter mouse spinal cord immunostained for CD11b. Scale bars = 50 μm for panels e–f. **(h)** Example Wiggle plots for mapped reads of *Oprm1* (red) in whole DRG (bottom plot) and in purified spinal microglia (top plot). Reads were registered for the partially overlapping microglial gene *Ipcef1* (gray) but not *Oprm1* exons 1–4 for microglia (top plot). In DRG, reads mapped to *Oprm1* exons 1 through 4 with little to no reads for *Ipcef1* (bottom plot). (**i**) Mapped reads for several cell types from RNA-seq transcriptome profiling of acutely purified spinal microglia in uninjured mice and in mice with Chronic Constriction Injury (CCI) of the sciatic nerve after 2 and 7 days. n = 2 independent sequencing experiments per group, consisting of pooled microglia from n = 15 mice for controls, n = 4 mice from CCI day 2 and n = 5 mice from CCI day 7. One-way ANOVA + Bonferroni (a, b) and Kruskal-Wallis (d).★ $P < 0.05$. Error bars are mean ± SEM. Overlaid points are individual subject scores. FPKM = Fragments Per Kilobase of transcript per Million mapped reads.

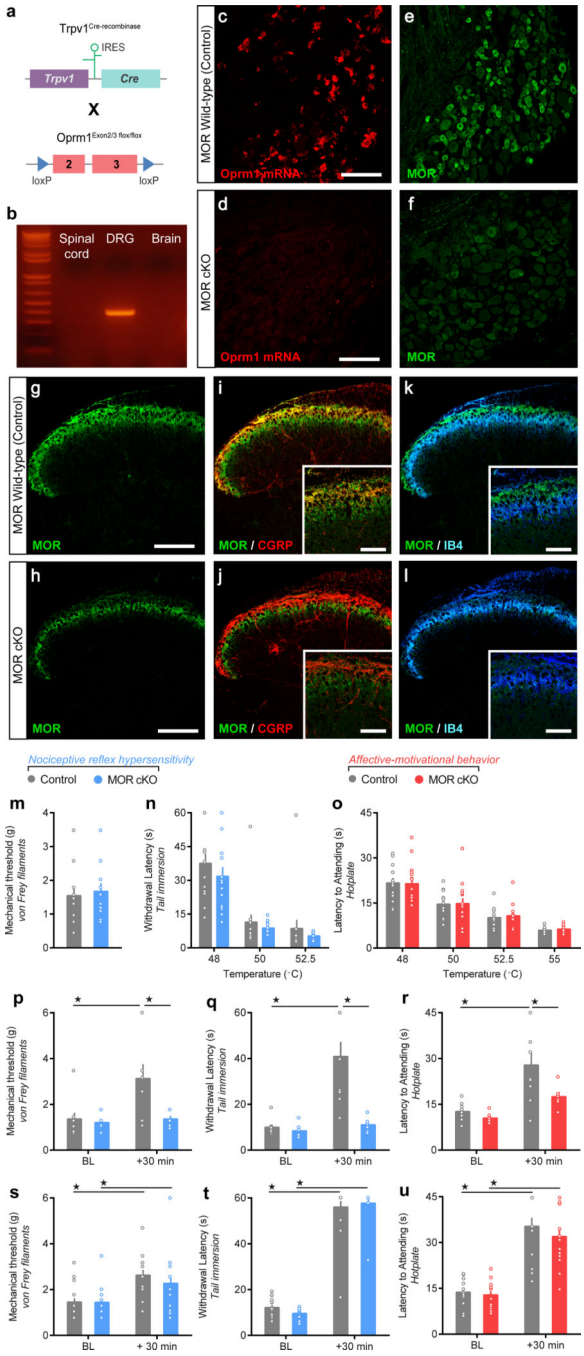

Figure 2. Conditional deletion of MOR from primary afferent nociceptors does not alter nociceptive behavior or reduce systemic morphine antinociception

(a) *Trpv1*^{Cre} mice were crossed with *Oprm1*$^{flox/flox}$ mice. Exons 2 and 3 of the *Oprm1* gene are flanked by loxP sites (triangles) and are excised in TRPV1 neurons expressing Cre recombinase. **(b)** PCR on genomic DNA showing excision of the floxed DNA fragment (363 bp). (**c,d**) *in situ* hybridization for *Oprm1* mRNA and (**e,f**) anti-MOR immunostaining in MOR cKO mice compared to littermate controls (n = 3 per genotype). (**g–j**) MOR co-immunostaining with CGRP in spinal laminae I and II outer in (i) control and (j) MOR cKO

mice. (**k,l**) MOR co-immunostaining with IB4 in spinal laminae I and II outer in (k) control and (l) MOR cKO mice. (**m–o**) Baseline nociceptive hypersensitivity or affective-motivational behavior to (m) von Frey filament mechanical stimulation of the hindpaw, (n) increasing water bath temperatures during tail immersion, or (o) increasing hotplate temperatures on the hindpaws between MOR cKOs (n = 15) and controls (n = 14). (**p–r**) Antinociception, resulting from an acute spinal morphine administration (1 μg, intrathecal) in MOR cKOs (n = 6) and controls (n = 9), in response to (p) von Frey mechanical stimulation ($F_{1, 13} = 5.132$, $P = 0.0412$), (q) 50 °C water tail immersion ($F_{1, 13} = 12.53$, $P = 0.0036$), and (r) 52.5 °C hotplate ($F_{1, 13} = 5.827$, $P = 0.0313$). (**s–u**) Antinociception, resulting from an acute systemic morphine administration (10 mg/kg, subcutaneous) in MOR cKO mice (n = 13) compared to controls (n = 17), when assessed by (s) von Frey mechanical filaments ($F_{1, 28} = 18.46$, $P = 0.0002$), (h) 50 °C water tail immersion ($F_{1, 28} = 18.78$, $P < 0.0001$), or (i) 52.5 °C hotplate ($F_{1, 28} = 12.95$, $P < 0.0001$). Repeated measures Two-way ANOVA + Bonferroni. ★ $P < 0.05$. Error bars are ± SEM. Overlaid points are individual subject scores. Scale bars = 50 μm, throughout. BL = baseline.

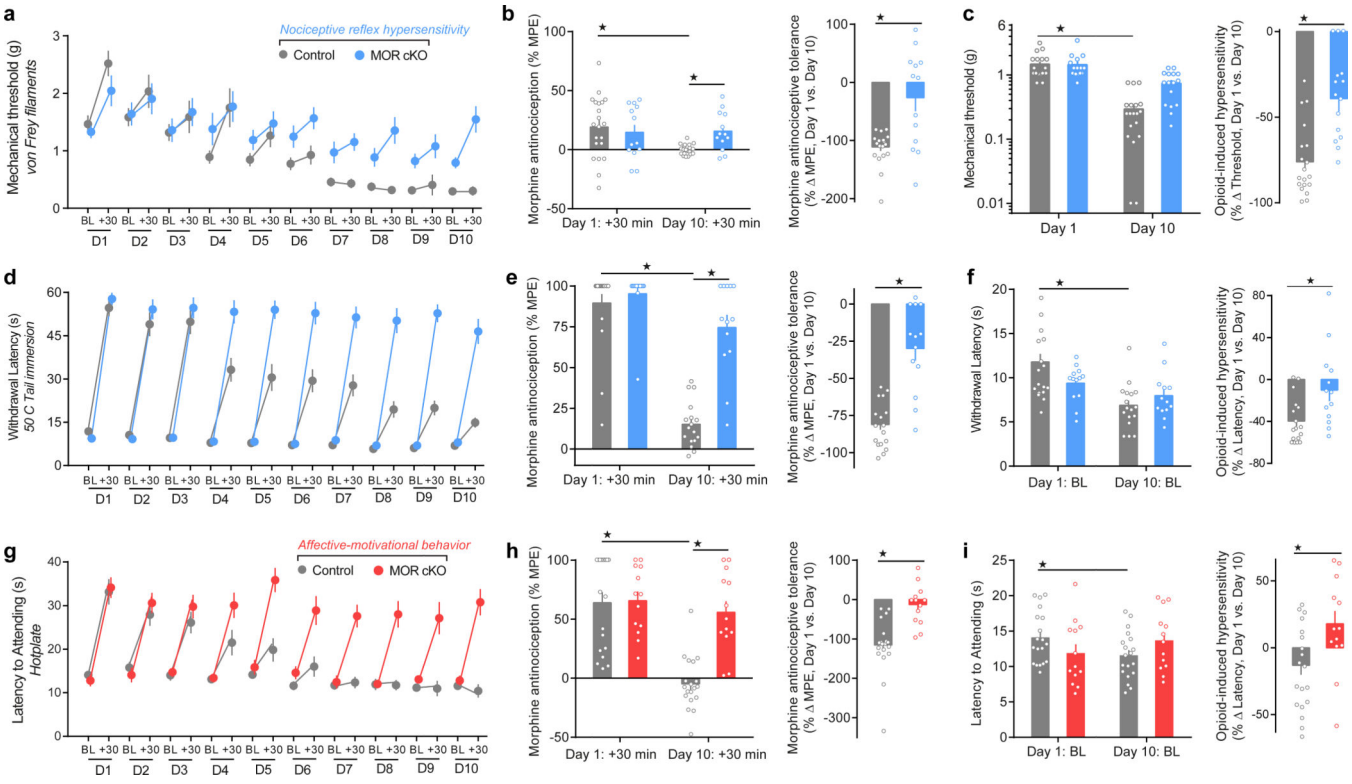

Figure 3. Conditional deletion of MOR from TRPV1 nociceptors prevents the onset of morphine antinociceptive tolerance and OIH

(**a,d,g**) Daily nociceptive behavior and opioid antinociception throughout a 10 day chronic morphine schedule (10 mg/kg, subcutaneous, once daily). Nociceptive behavior (pre-morphine BL timepoints only): von Frey: $F_{1, 30} = 9.863$, $P = 0.004$; tail immersion: $F_{1, 30} = 0.7311$; hotplate: $F_{1, 30} = 0.2581$, $P = 0.0615$. Antinociception (post-morphine +30 min timepoints only): von Frey: $F_{1, 30} = 4.812$, $P = 0.0367$; tail immersion: $F_{1, 30} = 19.74$, $P < 0.0001$; hotplate: $F_{1, 30} = 17.23$, $P = 0.0004$. (**b,e,h**) Antinociceptive tolerance: (*left panels*) Maximal possible effect (MPE) for morphine antinociception from the first administration (Day 1: +30 min) compared to the last administration (Day 10: +30 min) (von Frey: $F_{1, 30} = 7.621$, $P = 0.0097$; tail immersion: $F_{1, 30} = 28.27$, $P < 0.0001$; hotplate: $F_{1, 30} = 12.27$, $P = 0.0015$), and (*right panels*) the percent change for each subject. (**c,f,i**) OIH: (*left panels*) Percent change in the pre-morphine baseline nociceptive behaviors prior to the first administration (Day 1: BL) compared to the last (Day 10: BL) (von Frey: $F_{1, 30} = 6.13$, $P < 0.001$; tail immersion: $F_{1, 30} = 23.08$, $P < 0.0001$; hotplate: $F_{1, 30} = 5.163$, $P = 0.0304$), and (*right panels*) the percent change for each subject. Control, n = 19; MOR cKO, n = 13. BL = baseline. Student's *t* Test, two-tailed (right panels of b,c,e,f,h,i). Repeated Measures Two-way ANOVA + Bonferroni (a,d,g and left panels of b,c,e,f,h,i). ★ $P < 0.05$. Error bars are mean ± SEM. Overlaid points are individual animal scores. BL = baseline.

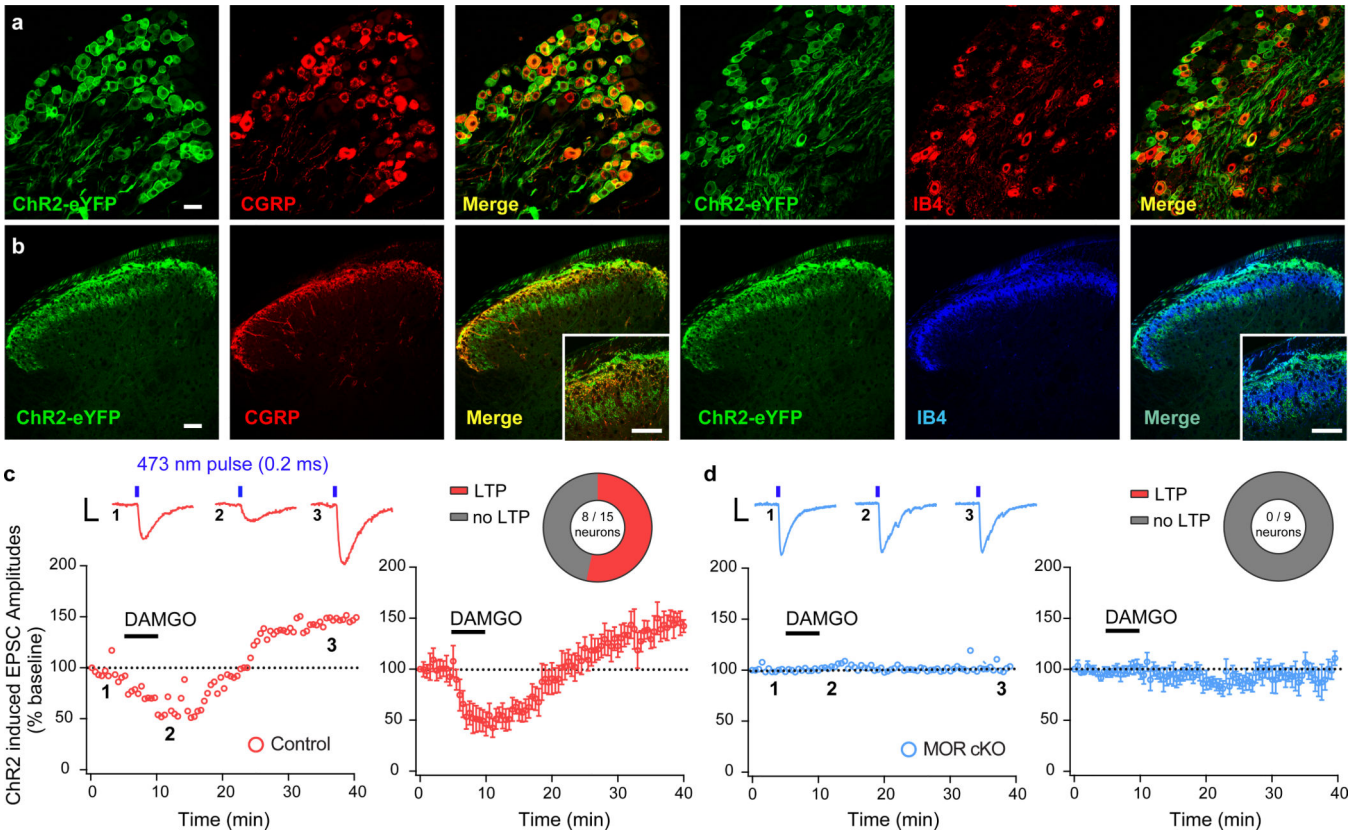

Figure 4. Opioid-induced spinal long-term potentiation (LTP) is initiated by presynaptic MOR in nociceptors

(**a,b**) MOR cKO mice crossed with a mouse line expressing Channelrhodopsin2 (ChR2-eYFP) in a Cre-dependent manner produces expression of ChR2-eYFP in *Trpv1*^{Cre}+ DRG nociceptor cell bodies and central terminals in the spinal cord dorsal horn. Scale bars = 50 μm, throughout. (**c,d**) Blue light-evoked (473 nm, 1.0 mW/cm^2, 0.2 ms, 0.05 Hz) EPSCs recorded in laminae I and II outer spinal neurons in slices from MOR cKO and littermate controls. Numbered inset traces correspond to individual EPSCs before, during, and after wash-out of bath applied DAMGO (500 nM; 5 min duration). Scale bar = 100 pA, 10 ms. (**c**) DAMGO-induced depression of EPSC amplitude and rebound LTP after washout (Control + LTP; n = 8 / 15 neurons) in control slices. (**d**) MOR cKO spinal neurons do not show DAMGO-induced depression of light-evoked EPSCs or rebound LTP upon DAMGO washout (n = 9 / 9 neurons). Error bars are mean ± SEM.

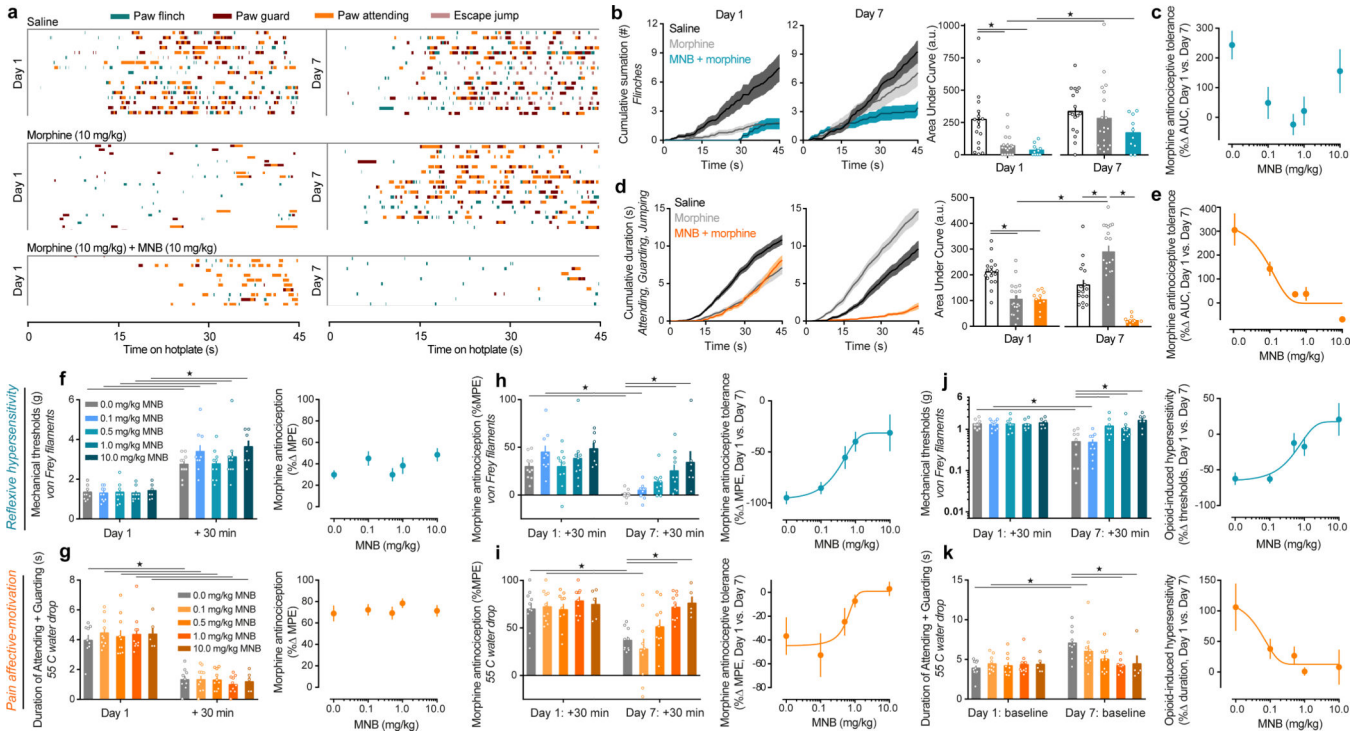

Figure 5. Pharmacological blockade of peripheral MOR by methylnaltrexone bromide (MNB) dose-dependently prevents the onset of morphine antinociceptive tolerance and OIH

(a) Temporal raster plot of nociception-induced sensory-reflexive and affective-motivational behaviors in an inescapable noxious environment (enclosed 52.5 °C hotplate). Each row displays the behavioral profile over 45 s for an individual mouse given either saline (n = 17), morphine (n = 19), or morphine + MNB (n = 10), on the first treatment (Day 1) and after chronic treatment (Day 7). **(b,c)** Summary of reflexive paw flinches in panel a: (b) cumulative summation and AUC analysis for Day 1 and Day 7 trials ($F_{2, 43} = 8.749$, $P = 0.0006$), and (c) the dose-response effect of MNB on morphine antinociceptive tolerance displayed as the percent change in AUC between trial days. **(d,e)** Summary of all affective-motivational behaviors in panel a: (d) cumulative summation and AUC analysis for Day 1 and Day 7 trials ($F_{2, 43} = 24.61$, $P < 0.0001$), and (e) the dose-response effect of MNB on morphine tolerance. **(f–k)** Effect of MNB co-administration at multiple doses on acute morphine antinociception for (f) mechanically-induced nociceptive paw flinches ($F_{1, 42} = 182.9$, $P < 0.0001$), (g) noxious thermal-induced paw attending and guarding ($F_{1, 39} = 279.9$, $P < 0.0001$), (h,i) antinociceptive tolerance (reflexive hypersensitivity: $F_{4, 42} = 3.54$, $P = 0.0141$; affective-motivational: $F_{4, 40} = 6.115$, $P = 0.0006$), and (j,k) OIH (reflexive hypersensitivity: $F_{4, 42} = 6.825$, $P = 0.0003$; affective-motivational: $F_{4, 40} = 3.619$, $P = 0.0131$). MNB doses 0.0 – 1.0 mg/kg, n = 10; MNB 10 mg/kg, n = 7 for reflexive tests and n = 5 for affective-motivational tests. Best-fit lines were generated following non-linear regression analysis based on the % MPE for each mouse. One-way ANOVA + Bonferroni (left panels of b,d,f–k). ★ $P < 0.05$. Error bars are mean ± SEM. Overlaid points are individual animal scores. PID = post-injury day.

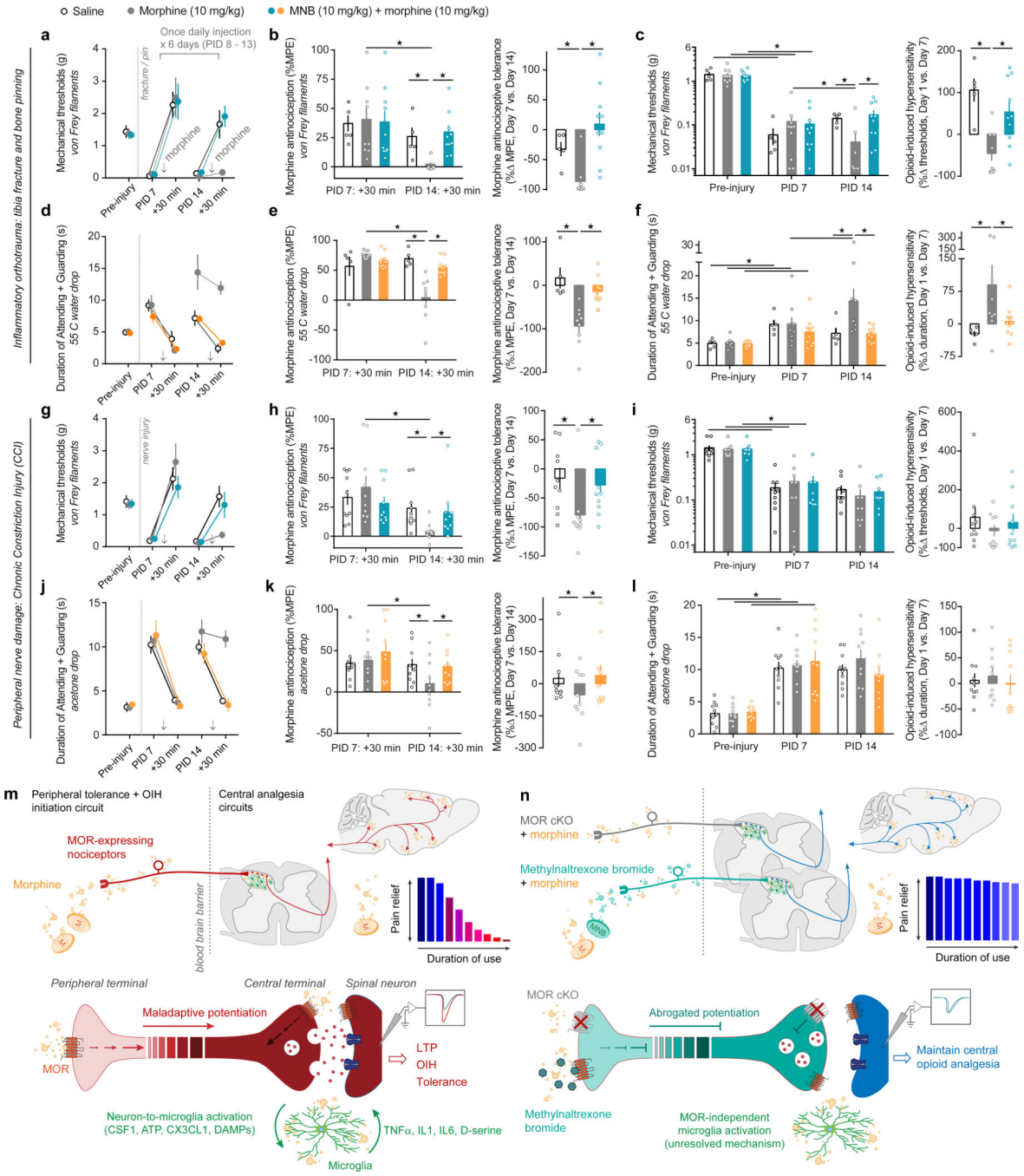

Figure 6. Combination therapy of morphine and MNB delivers long-lasting antinociception, without the onset of tolerance, during perioperative and chronic pain states

(a,d,g,j) Timecourse for (a,g) nociceptive hypersensitivity and (d,j) affective-motivational behaviors following an orthotrauma (tibia fracture and bone pinning), or a peripheral nerve injury (Chronic Constriction Injury, CCI), and the effect of chronic saline (n = 10 for fracture, n = 5 for CCI), 10 mg/kg morphine (n = 10 / injury model), or 10 mg/kg morphine + 10 mg/kg MNB (n = 10 / injury model) treatments. Treatments are first given on PID 7 and re-administered once daily until PID 14, with the exception that the Saline group is administered acute morphine only on PID 7 and PID 14. **(b,e,h,k)** Antinociceptive tolerance:

(left panels) Maximal possible effect (MPE) for morphine antinociception from the first administration (PID 7: +30 min) compared to the last administration (PID 14: +30 min) (Fracture: von Frey, F2, 21 = 2.05, P = 0.0023; 55 °C drop, F2, 21 = 6.084, P = 0.0082. CCI: von Frey, F2, 27 = 13.8, P = 0.0009; Acetone drop, F2, 27 = 5.976, P = 0.0213), and (right panels) the percent change for each subject. **(c,f,i,l)** OIH: (left panels) Percent change in the pre-morphine baseline nociceptive behaviors prior to the first administration (PID 7: BL) compared to just to the last (PID 14: BL) (Fracture: von Frey, $F_{2, 22} = 4.253$, $P = 0.0274$; 55 °C drop, $F_{2, 21} = 5.347$, $P = 0.0133$. CCI: von Frey, $F_{2, 27} = 0.05814$, $P = 0.9436$; Acetone drop, $F_{2, 27} = 0.4272$, $P = 0.6567$), and (right panels) the percent change for each subject. (**m,n**) Schematic detailing the influence of opioid-induced nociceptor maladaptive potentiation over CNS analgesic circuits to initiate tolerance and OIH. Conditional MOR deletion or MNB blockade of MOR signaling in nociceptors abrogates this potentiation, thereby maintaining opioid analgesic efficacy and reducing OIH. Two-way ANOVA + Bonferroni (for panels c,f,i,l two separate ANOVAs were run for Pre-injury vs. PID7, and PID7 vs. PID14). Student's *t* Test, two-tailed (right panels of b,c,e,f,h,i,k,l). ★ $P < 0.05$. Error bars are mean ± SEM. Overlaid points are individual animal scores. PID = post-injury day.